

# Immersion Cooling of a Simulated Electronic Chip Protruding into a Flow Channel

J. E. Leland\*

*U.S. Air Force Research Laboratory, Wright–Patterson Air Force Base, Ohio 45433-7251*

and

L. C. Chow†

*University of Central Florida, Orlando, Florida 32816-2450*

Nucleate boiling and critical heat flux from the top and side surfaces of a simulated electronic chip protruding into a rectangular channel has been studied. To ascertain the contributions of heat transfer from the sides and top of the simulated electronic chip, boiling from the sides was virtually eliminated by the use of a thin (0.025 mm) foil heater on top of a block of insulating material. It was found that single-phase heat transfer and critical heat flux are markedly greater for a surface protrusion height of 0.71 mm as compared to a flush surface. This increase was seen for flow velocities greater than 1 m/s and a subcooling of 20°C. The results are compared to that for a copper block heated from below under similar fluid and geometry constraints. These comparisons show that the vapor emanating from the upstream side of the copper block plays an important role in either decreasing or increasing the critical heat flux. Additional results were obtained for the copper block where heat transfer from the upstream side was obstructed. These results indicate that under some conditions of subcooling and flow rate an optimal amount of upstream side vapor production exists.

## Nomenclature

$c$	= specific heat of a solid
$c_p$	= specific heat at constant pressure
$D_h$	= hydraulic diameter based on wetted perimeter
$h$	= channel height
$h_{fg}$	= latent heat of vaporization
$h_p$	= heater protrusion height
$Ja$	= Jakob number, $c_p \Delta T_{\text{sub}} / h_{fg}$
$k$	= thermal conductivity
$L$	= simulated chip surface heated length
$Q_M$	= maximum power dissipation
$q$	= heat flux
$q_M$	= critical heat flux
$q_M^{**}$	= dimensionless critical heat flux
$R_a$	= International Organization for Standardization standard (ISO R468) for surface roughness
$Re$	= Reynolds number, $UD_h/\nu$
$T_b$	= bulk fluid inlet temperature
$T_n$	= surface temperature at location $n$
$T_{\text{sat}}$	= saturation temperature based on measured static pressure
$T_w$	= heated surface wall temperature
$t$	= heater thickness
$U$	= bulk mean velocity based on channel cross section
$We$	= Weber number, $\rho_f U^2 L / \sigma$
$w$	= channel width
$\Delta T_{\text{sub}}$	= subcooling, $T_{\text{sat}} - T_b$
$\Delta T_w$	= wall superheat, $T_w - T_{\text{sat}}$
$\nu$	= kinematic viscosity

$\rho$	= density
$\sigma$	= surface tension

## Subscripts

Flush	= flush heater surface
$f$	= liquid
$g$	= vapor

## Introduction

POWER electronics capable of handling hundreds of kilowatts are currently being developed for military and commercial applications.<sup>1</sup> As the heat-dissipation rates of these devices exceed the practical limits of air and single-phase liquid cooling, more aggressive approaches such as direct immersion two-phase cooling become attractive. The study of direct immersion nucleate boiling and critical heat flux (CHF) associated with electronic chips has been the focus of numerous studies.<sup>2–5</sup> CHF is the term given to the point at which a transition from nucleate boiling to film boiling occurs. This transition is marked by a large and rapid temperature excursion that is generally accompanied by burnout of the heating element. Myriad flow geometries and a large range of fluid conditions were included in these studies. For the rectangular flow channel substantial studies have been performed,<sup>6–8</sup> and were concerned with heat transfer from heat sources that are flush with the flow channel wall. Gu et al.,<sup>9</sup> however, discovered that CHF decreases markedly if the heated surface is not maintained flush with the flow channel wall. This degradation occurred for surface recess and protrusion heights less than 0.1 mm. Because it is difficult to maintain flushness after repeated thermal cycling under closely controlled laboratory conditions, the same problem will exist for actual electronic chip cooling applications.

Leland and Chow<sup>10</sup> and Leland<sup>11</sup> studied the effect of heated surface protrusion height (–0.127 to 0.635 mm) on forced convective boiling and CHF for flow velocities of 1–4 m/s and subcoolings of 20 and 35°C. Heated surface refers to the top surface of the protruding block. In their experiments, a copper block heated from below was used to simulate an electronic chip protruding into a rectangular flow channel. Boiling

Received Oct. 20, 1997; revision received Feb. 24, 1998; accepted for publication Feb. 25, 1998. This paper is declared a work of the U.S. Government and is not subject to copyright protection in the United States.

\*Research Engineer, Power Division. E-mail: lelandje@wl.wpafb.af.mil. Member AIAA.

†Professor, Department of Mechanical and Aerospace Engineering. Associate Fellow AIAA.

occurred predominantly on the front face (the upstream face normal to the direction of flow), top, and rear (downstream) face of the block. They found that for a given protrusion height, as compared to the case where the block was flush, the CHF (based on exposed area) was 1) reduced at low velocities, 2) equal at some intermediate velocity, and 3) increased at higher velocities. As the protrusion height was increased, the velocity at which the protruded surface CHF equaled the flush surface CHF decreased. Also, CHF increased with increasing protrusion height for velocities greater than the break-even velocity. The net increase in CHF was unexpected and it was suspected to be, in part, a result of the strong interaction between vapor emanating from the front face and that from the top of the block. Furthermore, a flow instability phenomenon occurred for heater heights of 0.457 and 0.635 mm. In both cases, the instability occurred at a velocity and subcooling of 2 m/s and 20°C, respectively.

McGillis et al.<sup>12</sup> also investigated the effect of heated surface protrusion height (0.8–2.4 mm), for velocities of 9.6–103.9 cm/s and subcoolings of 20–40°C. They found a reduction in CHF (based on exposed area), for all combinations of velocity, subcooling, and surface height. Because their results were obtained for flow velocities of about 1 m/s or less, their results qualitatively agree with those of Leland and Chow<sup>10</sup> and Leland.<sup>11</sup> Nonetheless, their data were obtained for 10 heat sources in-line and, thus, little insight into the controlling mechanisms of CHF was obtained. The combined effects of protrusion height and channel height were studied by Gersey and Mudawar<sup>13</sup> for a series of nine in-line heat sources. They obtained results for a protrusion height of 1 mm, channel heights of 2 and 5 mm, flow velocities of 13–400 cm/s, and subcoolings of 3–36°C. Their results also qualitatively agree with those of Leland and Chow<sup>10</sup> and Leland<sup>11</sup> as summarized earlier. Gersey and Mudawar<sup>13</sup> also report that nucleation of the most upstream heat source was inhibited for flow velocities of about 1 m/s. This phenomenon is believed to be related to the instability phenomenon described by Leland and Chow<sup>10</sup> and Leland.<sup>11</sup> Because their results were obtained for a single protrusion height and a series of heat sources, there is still a need for greater understanding of the controlling mechanisms of CHF for protruded surfaces.

Thus, the present effort was undertaken to separate the contribution of heat transfer from the sides of the protruding block from that of the top of the protruding block and understand how each relates to the CHF. Experiments were also conducted to determine if the flow/boiling heat transfer instability could be prevented without diminishing the enhanced heat transfer characteristics of the protruded chip configuration.

### Experimental Apparatus

The experimental apparatus consists of four basic components: 1) The flow loop, 2) the flow channel, 3) the test heater enclosure, and 4) the heater section. A dielectric fluorocarbon, FC-72 (3M Industrial Chemical Products Division) was used as the heat transfer fluid. Details of the flow loop, flow channel, and heater enclosure have been described previously by Leland and Chow<sup>10</sup> and Leland.<sup>11</sup> The heater enclosure is shown installed in the flow channel in Fig. 1. Two different heater assemblies were used: 1) A resistively heated thin foil and 2) a copper block heated from below. Details of the latter design have been previously described.<sup>10,11</sup> The thin foil heater was designed such that boiling would occur only from the top of the protrusion. This heater was made of 0.025-mm-thick Monel 400 mounted on top of a low thermal conductivity (0.29 W/m-K) G-7, (a laminated fiberglass cloth material), block as shown in Fig. 2. The Monel foil was soldered to 0.25-mm-thick copper strips that were slit lengthwise to provide voltage sensing taps at the heater. The resistance of the copper leads was negligible compared to the foil. Heat conduction through the leads was suppressed by bending the copper leads inward so that they would be insulated by additional pieces of G-10

(a more dense, more conductive, easier to machine version of G-7).

Five 0.076-mm-diam wire, type T thermocouples were used to monitor the temperature of the foil. Four of these are imbedded in grooves on the top of the G-7 block. Figure 3 shows that three of the four are used to measure the streamwise temperature variation, whereas two were used to measure the spanwise variation. The grooves were carefully contoured to ensure that the thermocouple beads were as close as possible to the backside of the foil. The foil was epoxied to the G-7 block using Omegabond 200 epoxy (Omega Engineering, Inc.), thus ensuring good thermal contact between the thermocouples and foil. A cure time of 8 h at 120°C was found to be optimal. It is estimated that the thermocouple beads were separated by a thin layer of epoxy no more than 0.04 mm thick. The fifth thermocouple was located 0.25 mm below the center of the surface and was used to estimate heat loss through the G-7.

The copper block test section is the same as described by Leland and Chow<sup>10</sup> and Leland,<sup>11</sup> with the exception of a small block of insulating material added to the front face of the cop-

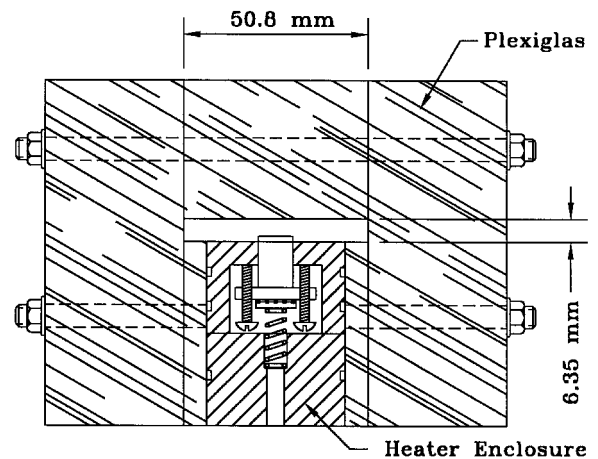


Fig. 1 Flow channel cross section with test heater.

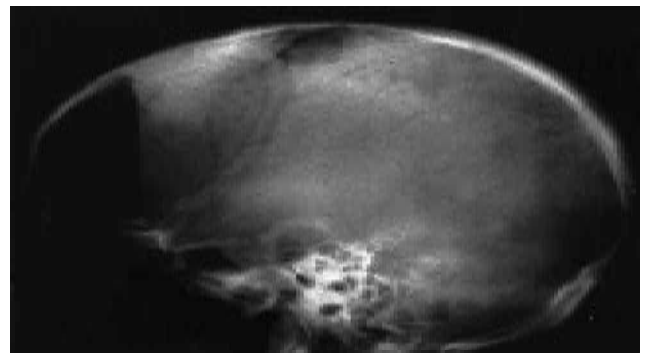


Fig. 2 Thin foil heater assembly.

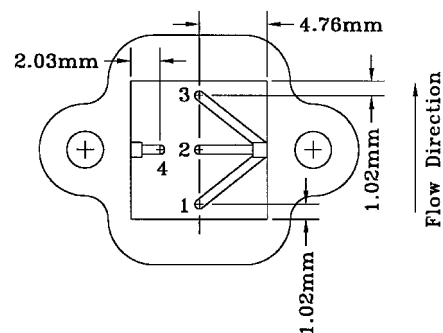


Fig. 3 Foil heater thermocouple locations.

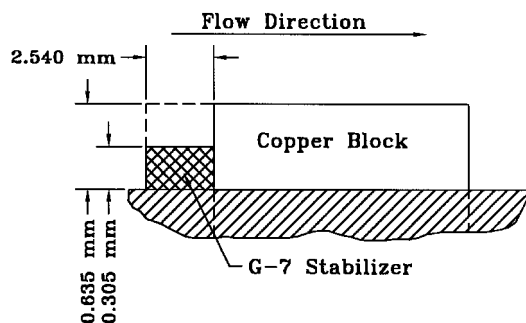


Fig. 4 Front-face insulator details.

per block. The insulating material covered either half or all of the front face of the block and eliminated boiling from the covered portion. Figure 4 shows the exact dimensions and location of these alternate pieces of insulating material. The surface of the Monel foil was prepared in the same way as described by Leland and Chow,<sup>10</sup> and had a surface roughness  $R_a$  of only 4 nm as measured with a Taylor-Hobson surface profilometer. Eight measurements at various surface locations showed that the surface roughness was uniform to within  $\pm 1$  nm.

### Uncertainty Analysis

A Hewlett Packard 3852A data acquisition system was used to make all voltage and temperature measurements. This device has a resolution of 0.02°C and rated accuracies of 0.5 and 0.65°C for thermocouple types K and T, respectively. The data acquisition unit and type T thermocouples were compared to a precision digital resistance temperature detector (RTD) (0.03°C rated accuracy) over the range of interest, and the system accuracy was found to actually be within 0.3°C. Thus, no further corrections were made. The uncertainties associated with the flow channel and the tests with the copper block/thick film resistor test section have been previously described by Leland and Chow.<sup>10</sup> For convenience, the uncertainties in CHF for the copper block test section were reported as 13.4, 7.8, and 6.9% for heat fluxes of 34, 85, and 132 W/cm<sup>2</sup>, respectively. The uncertainties associated with the thin foil heater test section are described next.

For all tests with the foil heater, CHF was calculated from the electrical power measurement. The standard Kline and McClintock<sup>14</sup> approach to random uncertainty calculation yields an uncertainty of 0.27%. A one-dimensional heat conduction assumption was made to estimate the heat loss from the back of the foil through the G-7 substrate. This method predicted less than 1% heat loss for heat fluxes greater than 15 W/cm<sup>2</sup>. Because of assuming one-dimensional heat conduction, this method may underestimate the heat loss but, the error would still be small. Thus, no correction was made to the foil heater results.

The surface thermocouples fluctuated by as much as 1°C during testing, depending on the location of the nucleation sites. The thermocouples would vary most when near the edge of a patch of advancing nucleation sites. Nucleation occurs first at the most downstream portion of the heater surface. As power to the heater is increased this small patch of nucleation sites expands toward the upstream edge of the heater surface. The upstream border of the patch of nucleation sites is not stable and, therefore, temperature fluctuations are greatest at this location. Thermocouples well within the zone of nucleation were the most steady, fluctuating only 0.3°C. Kenning<sup>15</sup> has shown that large errors may occur in the surface temperature measurement of thin foil heaters. These errors are caused by the large variation in heat flux below a single bubble at a nucleation site. The average heat flux at a given nucleation site also varies greatly from that between nucleation sites. Kenning measured a spatial temperature variation (over one nucleation

site domain of influence), of 26°C for water boiling at 10 W/cm<sup>2</sup> on a stainless-steel foil 0.13 mm thick. It must be noted that in Kenning's experiments, most of the nucleation sites were separated by a distance of more than three bubble diameters.

Using a conduction model, Kenning was able to predict the temperature variation. Using Kenning's model and characteristic bubble size and spacing information from the current experiments, a maximum spatial temperature variation of 6.0°C is obtained. This value is overpredicted because the foil heater of the present study is in good thermal contact with the G-7 substrate. Although the substrate is of low thermal conductivity, it will still act in reducing site-to-site thermal gradients. Furthermore, the present results are much lower than those reported<sup>15</sup> because the high bubble density under high flux conditions creates a more uniform heat flux pattern on the surface. Also, maximum bubble sizes are much smaller under subcooled, forced flow conditions, further damping thermal gradients. Thus, the measured fluctuation of 1°C is considered reasonable. More details of the analysis are given by Leland.<sup>11</sup>

Leland and Chow<sup>10</sup> and Leland<sup>11</sup> performed the same analysis for the copper block heater and found that spatial temperature variations are completely damped at about one bubble diameter below the surface. This translates into a distance of no more than 0.2 mm. Thus, there is no impact on the measurements obtained for the copper block test section.

### Experimental Results

Results have been obtained for two heater configurations: 1) A thin foil heater and 2) a copper block heated from below. The effects of large-scale (0.12-mm amplitude ripples) surface roughness and protrusion height were studied for the thin foil heater configuration. The effects of protrusion height and insulation of the front face were studied for the copper block heated from below. Data were obtained for velocities of 1–5 m/s and subcoolings of 20–35°C, respectively. However, foil heater data were not obtained for a subcooling 35°C because of the short lifetimes of the foils.

#### Foil Heater Test Section

Because of the complexity of the thin foil heater configuration, many failures were experienced before an optimal assembly procedure was found. As a result, there are few quantitative results for the smooth foil and some of the results for the rippled foil were derived from single sample measurements. The qualitative results were significant, however, and are reported herein.

Incipient temperature overshoot was generally much higher for the thin foil configuration than previously noted<sup>10,11</sup> for the copper block configuration. A maximum incipient overshoot of 20°C was measured for the smooth foil, 20°C subcooling, and a velocity of 1 m/s. Temperature overshoot was negligible for the majority of tests conducted with the copper block test section and was less than 1°C for most other cases. The most likely explanation is that the very thin foil did not distribute the heat through itself nearly as well as the thicker copper block test section. For the copper block the surface temperature distribution varied by only 2.2°C. Thus, similar conditions existed over the surface and incipience occurred at the rear-most edge of the heater where the thermal boundary layer was first sufficient for nucleation. For the foil heater, large thermal gradients could exist because of the poor lateral conduction of heat (Fig. 5). Thus, incipience could occur more randomly over the surface at certain hot spots. Even if incipience occurred at a single point, substantial increases in heat could be necessary before more significant nucleation of the surface occurred. Incipient overshoot generally decreased with velocity, which is in agreement with the trend noted for the copper block test section.<sup>10</sup>

Figure 5 shows how the surface temperature progresses with heat flux for a typical case. The temperatures are plotted in

reference to the upstream thermocouple  $T_1$  (see Fig. 3 for the key to thermocouple numbers). It may be seen that at the lowest heat flux the downstream thermocouple  $T_3$  is the hottest with the center thermocouple  $T_2$ , slightly cooler and the spanwise thermocouple  $T_4$ , the coolest. This trend is obviously expected with the possible exception of the spanwise temperature. As heat flux increases, nucleation occurs at the downstream thermocouple and a sharp drop in temperature ensues. With further increases in heat flux, nucleation occurs at the center and side locations and  $T_3$  drops further because of more complete nucleation. Throughout the nucleate boiling regime, 15–25 W/cm<sup>2</sup>, the streamwise variation in temperature is very small, <1°C. As the CHF is approached, the downstream location begins to rise dramatically with temperature as dryout occurs and localized film boiling ensues. The center location also rises in temperature as CHF is approached, but less dramatically. The fact that dryout occurs at the most downstream location first, supports the dryout model proposed by Haramura and Katto<sup>16</sup> and adapted to the present geometry by Mudawar and Maddox.<sup>6</sup>

Figure 5 also shows that the side thermocouple remains about 2°C cooler throughout the single-phase and boiling regimes. Because the streamwise variation in temperature is less than 1°C, the relatively larger spanwise variation indicates that there is significant inflow of liquid from the sides of the heated surface. This was witnessed to some degree by the departing vapor bubbles being swept toward the streamwise centerline of the heater surface, particularly toward the downstream portion of the heater surface.

The CHF for the foil heater was generally 25% lower than that of the copper block heater for the same flow velocity and subcooling. This is in agreement with pool boiling studies that have shown that below a critical heater thickness, pool boiling CHF begins to decrease with decreasing thickness. Sharp<sup>17</sup> made an exhaustive study of pool boiling from various materials of small thickness and found that boiling heat transfer coefficient was proportional to the material's thermal effusivity  $\sqrt{\rho c k}$  and thickness. Sharp's findings have been confirmed by many other investigators for pool boiling but flow boiling data are sparse. A comprehensive literature survey and discussion on the effects of heater thickness is given by Leland.<sup>11</sup>

The quantity  $t\sqrt{\rho c k}$  governs the ability of the heater to mitigate a sudden hot spot. As  $t\sqrt{\rho c k}$  decreases below the critical value, the heat below an intermittently created dry spot is not as effectively distributed to other parts of the surface where effective boiling heat transfer continues. As a result the heater below the dry spot gets even hotter and eventually reaches the

Leidenfrost temperature where wetting cannot occur. For the present experiments CHF was found to be very sensitive to small imperfections in the foil surface. These imperfections created premature dryout and CHF could occur even at the leading edge of the heater. Dry out propagated so slowly that complete dryout of the surface took more than 5 s as opposed to the copper surface where complete dryout occurred in a fraction of a second. This implies that the nonuniform nature of heat generation within electronic chips could have a significant impact on CHF. This problem may not exist for power electronics where cooling is accomplished through a copper base typically 2.5 mm in thickness.

An example of more substantial surface imperfections is rippling of the foil caused during assembly. Results for the rippled surface in the flush condition are substantially lower than those obtained for a smooth surface. Reductions in CHF of 18 and 24% over the smooth foil were measured for flow velocities of 1 and 2 m/s, respectively. The ripples had an amplitude of no greater than 0.12 mm and a nonuniform distribution and frequency. Stating that the rippled surface is flush with the flow channel wall is, of course, questionable. However, most of the roughness elements were less than 0.02 mm in amplitude and, thus, were of the same order as the protrusion height measurement accuracy.

Results were also obtained for a protrusion height of 0.71 mm for the rippled surface only. Leland and Chow<sup>10</sup> and Leland<sup>11</sup> previously found that for the copper block test heater and a given protrusion height, CHF would be lower than that for the flush condition at low flow velocity. As flow velocity was increased, CHF for the protruded condition would be equal to and then greater than the value of CHF for the flush condition. As  $h_p$  increased, the increase in CHF over the flush condition also increased. It is important to note that CHF was based on the exposed area of the protruding copper block. Thus, any increase was actually an enhancement of the boiling mechanism and not merely an area augmentation. Figure 6 compares the current foil heater data ( $h_p = 0.71$  mm), to previously obtained copper block heater data.<sup>10</sup>

The trend for the foil heater is somewhat different than that for the copper block. The reduction in CHF at low velocity for the foil heater is much less than the same reduction for the copper block. However, the gain in CHF at higher velocities for the foil heater is less than the gain for the copper block. This latter effect may be because of the rippled surface. Finally, Leland and Chow<sup>10</sup> and Leland<sup>11</sup> reported a flow instability for the protruded copper block, 20°C subcooling, and a flow velocity of 2 m/s. The disappearance and reappearance

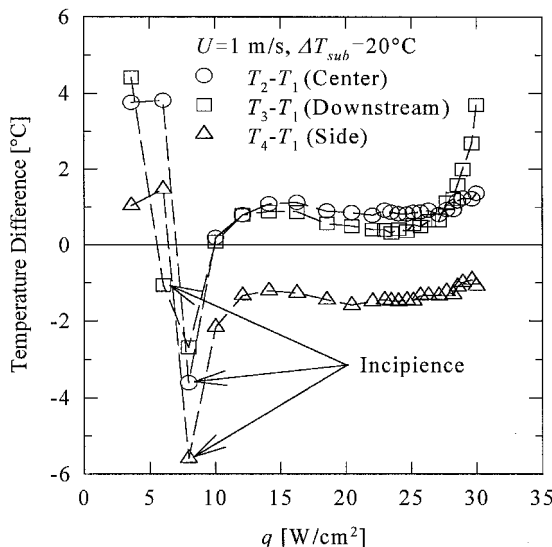


Fig. 5 Variation of thin foil heater surface temperatures relative to  $T_1$  with heat flux.

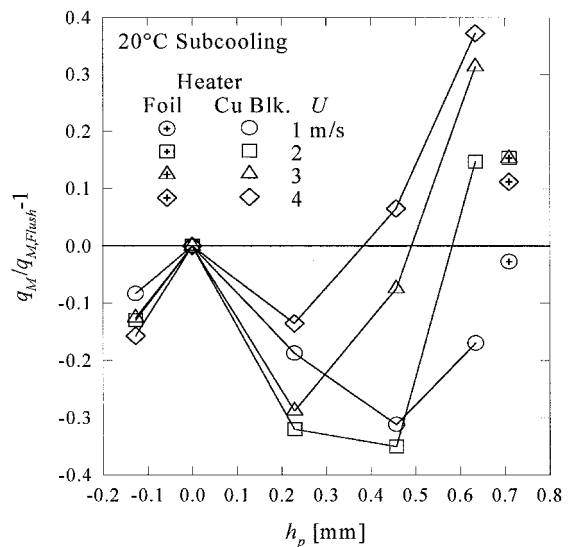


Fig. 6 Comparison of CHF with heater height and velocity for thin and thick heaters.

of a sheet of vapor emanating from the front face of the protruding copper block was evidence of this instability. The surface temperature of the copper block also fluctuated with the sheet of vapor and at an amplitude of more than  $1^\circ\text{C}$ . The instability phenomenon was completely absent during tests of the protruded foil heater.

The preceding observations are explained by the lack of any boiling from the front face of the protruding foil heater block. A smooth, uniform bubble layer evolved on the top surface of the foil in a fashion similar to that described by Leland and Chow<sup>10</sup> for the flush copper block surface. For the protruding foil heater block the bubble layer was thinner than that of the flush condition for a given velocity. This is because higher velocity liquid near the top surface for the protruded case pushes the vapor bubbles downstream at a greater rate. The higher velocity liquid is a result of a redeveloping boundary layer. This higher-velocity liquid also improves the liquid supply mechanism for nucleate boiling and inhibits the onset of CHF. Mudawar and Maddox<sup>6</sup> used flow visualization results to describe two liquid-supply mechanisms for the flush condition: 1) A low-speed ( $<2$  m/s) and 2) a high-speed ( $>2$  m/s) mechanism. For  $U < 2$  m/s, the liquid is fed tangential to the surface from the upstream edge to the downstream edge. As a result liquid supply to the most downstream sites is impeded and CHF is initiated at the most downstream portion of the heated surface. The vapor blanket increases in thickness with  $L$  for this case. For  $U > 2$  m/s, the vapor blanket is uniform in thickness and liquid feeds from above.

The same mechanisms likely exist for the protruded heater. Therefore, at low bulk flow velocities the previously mentioned vapor sheet for the copper block heater impeded the flow of the higher velocity fluid and, thus, diminished any gains in CHF. At higher bulk flow velocities the vapor sheet created a flow pattern that caused vapor above the surface to be swept up and toward the streamwise centerline. This mechanism helped to improve the liquid supply to the copper block heater surface for  $U > 2$  m/s. For the foil heater, there is no vapor sheet to create favorable flowfields and, thus, the enhancement is caused only by a redeveloping velocity layer. The absence of any flow instability is also owed to the lack of any boiling from the front face of the foil heater block.

### Copper Block Test Section

For an actual computer chip, heat is generated from within and distributed somewhat evenly over its exposed faces. Therefore, the copper block test heater more closely models the actual situation. It was surmised that if boiling from the front edge could be eliminated, the full enhancement of a redeveloping velocity layer would be realized. The loss of heat transfer area would amount to only 5% for the maximum protrusion height investigated. The area advantage of the remaining three sides would still be enjoyed.

Elimination of boiling from the front face was accomplished by the installation of a small block of G-7 laminated plastic (Fig. 4). The effects of the G-7 block were studied for a protrusion height of 0.635 mm. This included two cases, 100 and 48% coverage of the front face. Figure 7 shows that both sizes of the G-7 plastic insulator did indeed stabilize the boiling heat transfer at the  $20^\circ\text{C}$  subcooling, 2-m/s flow velocity condition. For example, the cases with insulators show no discontinuity in the boiling curve. The instability phenomenon has been described in depth by Leland and Chow<sup>10</sup> and Leland.<sup>11</sup> The aforementioned flow and heat transfer instability was completely absent. It was previously shown<sup>10</sup> that the instability did not occur for protrusion heights less than 0.457 mm. Therefore, an even thinner piece of insulating material may suffice in stabilizing heat transfer for this condition. Figure 8 shows the effect of the front-face insulators on CHF. The reduction in CHF at 1 m/s was sharply reduced. Besides elimination of the instability condition, further heat transfer enhancement was not realized for velocities greater than 1 m/s. Full coverage of the front face

yields essentially zero net heat flux gain over the flush condition for a subcooling of  $20^\circ\text{C}$ . It should be remembered that increased power dissipation is still realized. For  $35^\circ\text{C}$  subcooling, heat flux is actually decreased. For 48% coverage the flow instability remained absent and better heat transfer results were obtained, particularly for  $20^\circ\text{C}$  subcooling. The opposing effects of the insulators for  $U = 1$  m/s and  $U > 1$  m/s can be explained by the existence of the two different liquid supply mechanisms previously described. Remember that for  $U > 2$  m/s, the vapor blanket is uniform in thickness and liquid feeds from above. For this regime, CHF is much less sensitive to the heated length  $L$ .

Because boiling from the front face creates a vapor blanket that obstructs the flow tangential to the top surface, it is easy to understand how CHF is enhanced by installation of the insulator. For  $U > 2$  m/s, the flow mechanics created by the front-face boiling must make a significant contribution to heat transfer as evidenced by the degradation of CHF with installation of the insulators. For example, a reduction of 26 W occurred by the total elimination of boiling from the front face for the case of  $\Delta T_{\text{sub}} = 20^\circ\text{C}$  and  $U = 4$  m/s. With an area loss of only  $6.0\text{ mm}^2$ , this translates into a heat flux of  $430\text{ W/cm}^2$  if heat transfer from the other surfaces is assumed to remain constant. Such a high heat flux is certainly impossible for this configuration. Therefore, the liquid supply mechanism for the

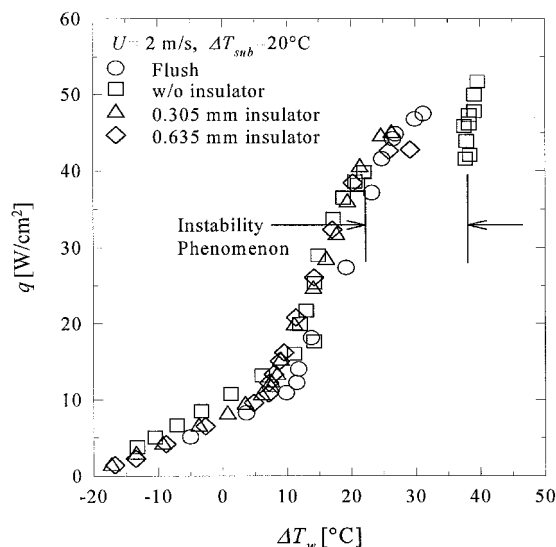


Fig. 7 Behavior of boiling curve with and without insulators.

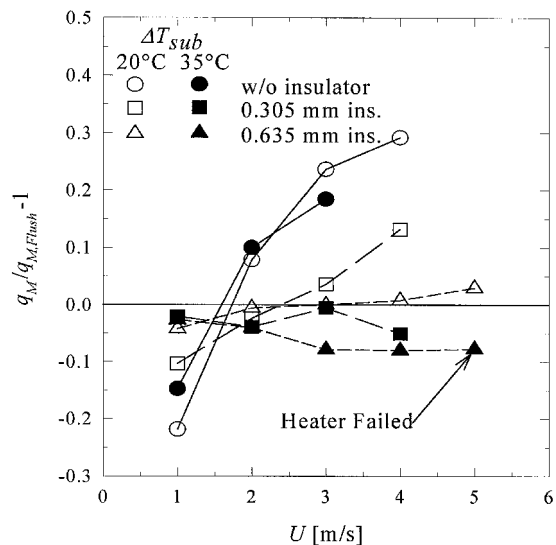


Fig. 8 Insulated and noninsulated protruding heater CHF compared with flush heater CHF.

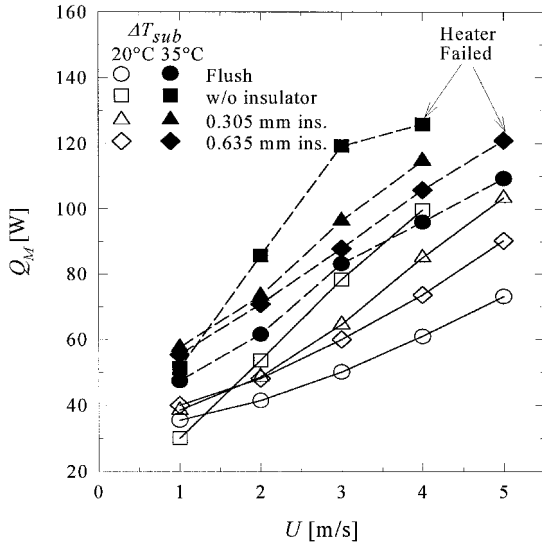


Fig. 9 Power dissipation vs velocity for heaters with and without insulators.

other surfaces must be enhanced in some way by the vapor sheet emanating from the front face. One possibility may be that condensing bubbles above the surface draw cool liquid in from the sides to feed the nucleation sites. The blunt face of the protruding block causes the vapor generated on this face to be projected up. This vapor is outside of the thermal boundary layer and in the presence of cooler liquid where it is more likely to condense.

For 35°C subcooling, similar trends are noticed, but the results relative to the flush condition (Fig. 8), generally fall below the results for 20°C subcooling and  $U > 2$  m/s. The reverse is true for  $U < 2$  m/s. This can be explained by first noting that as velocity increases, the contribution of single-phase heat transfer becomes a smaller percentage of the total heat transfer near CHF. At 35°C subcooling the single-phase contribution is greater than at 20°C subcooling. Furthermore, unlike water, FC-72 has a low latent to sensible heat ratio, 3.8 and 2.2 for  $\Delta T_{\text{sub}} = 20$  and 35°C, respectively. Thus, the results for 35°C subcooling are heavily biased toward single-phase heat transfer and augmentation or degradation of boiling heat transfer will have a lesser effect. For the case of no insulator this is easily seen. The effect of the insulator is to reduce or eliminate the vapor sheet emanating from the front face. As a consequence, the single-phase and overall heat transfer is reduced, although the boiling heat transfer may be augmented.

For  $U = 4$  m/s and  $\Delta T_{\text{sub}} = 20^\circ\text{C}$ , increases of 21, 39, and 64% over  $Q_{M,\text{Flush}}$  were obtained for the 0.635-mm insulator, 0.305-mm insulator, and no insulator cases, respectively. These percentages are much higher than the heat flux-based percentages. However, as mentioned before, power dissipation is the real goal of electronics cooling. Power dissipation is simply the product of heat flux and area. If CHF increases with heater height, this product increases at a greater rate because an exposed area also increases. Figure 9 illustrates how dramatically power dissipation increases with velocity.

### Correlation of CHF Results

Correlations of the flush and protruded surface cases have been obtained for the copper block test section data. Data for the copper block test section with front face insulation are not considered.

#### Flush Surface

Leland and Chow<sup>18</sup> obtained a correlation for a flush surface straight channel flow that fit the data with a mean absolute error of only 5.7%. The resulting equations were

$$q_M^{**} = 0.101 We^{-0.481} \quad (1)$$

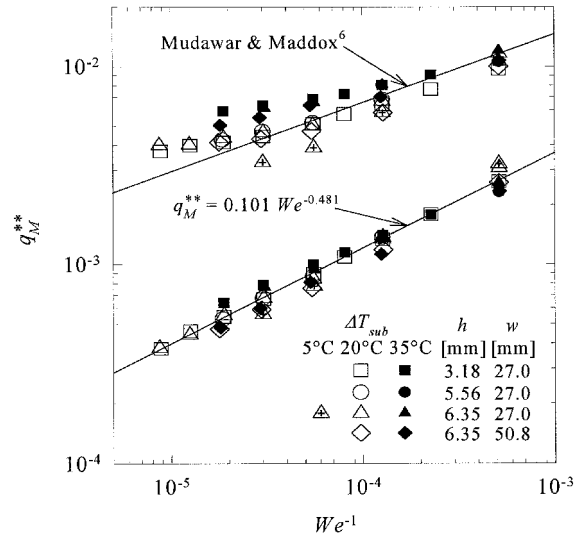


Fig. 10 Comparison of new straight channel data with correlations.

where

$$q_M^{**} = \frac{q_M / \rho_g h_{fg} U}{(\rho_f / \rho_g)^{0.167} (L/D_h)^{0.310} Re^{0.336} [1 + 4.561 Ja^{1.392}]} \quad (2)$$

This correlation is valid for  $w = 27.0$  mm,  $h = 3.18$ – $6.35$  mm,  $U = 1$ – $7$  m/s,  $\Delta T_{\text{sub}} = 5$ – $35^\circ\text{C}$ , and  $\rho_f / \rho_g = 77.7$ – $123.3$ . Figure 10 shows the data of the present test section (diamonds), and the previous straight channel data<sup>18</sup> plotted against the preceding correlation. The correlation fits the sum of the previous data and the current flush chip data with a mean absolute error of 8.5%. The present test section is within the range of validity of the preceding correlation except for the channel width that is 50.8 mm. Because the previous channel width, 27.0 mm, was significantly greater than the heater width, channel width is not considered to be a governing factor in the reduced quality of fit. Bias errors are not considered to be any different than for the previous test sections because the construction is very similar and measured heat losses are similar. Because a fit of the data to a mean absolute error of 8.5% is still considered good, no attempt was made to fit new exponents to the preceding correlation.

For comparison the data are also plotted against the theoretically obtained correlation of Mudawar and Maddox.<sup>6</sup> It is interesting to note that the Mudawar and Maddox correlation fits the data for the current geometry very well within the best-fit range, i.e.,  $10^{-4} < We^{-1} < 10^{-2}$ , of that correlation. This may be because the current test section geometry is closer in dimension to that of Mudawar and Maddox, where  $h = 12.7$  mm and  $w = 38.1$  mm.

### Correlation of Protruded Surface CHF Results

Correlation of the CHF results was attempted for the protruded surface results only because these are considered to be the only quantified results of interest to cooling system designers. Furthermore, the complex nature of CHF vs protrusion height makes correlation of these results difficult enough. For the same reasons, correlation of the insulated face cases was not attempted. Figure 11 shows how the data for  $-0.127$  mm  $\leq h_p \leq 0.635$  mm compare to Eqs. (1) and (2). As may be seen, a general trend with velocity or subcooling is absent.

Experimental data for the single-phase heat transfer coefficient of similar geometries have been correlated as a function of several variables. Roeller and Webb<sup>19</sup> used the flow channel dimensions  $h$  and  $w$ , and the heated protrusion dimensions, protrusion width  $w_p$ , protrusion length  $l_p$ , and the protrusion

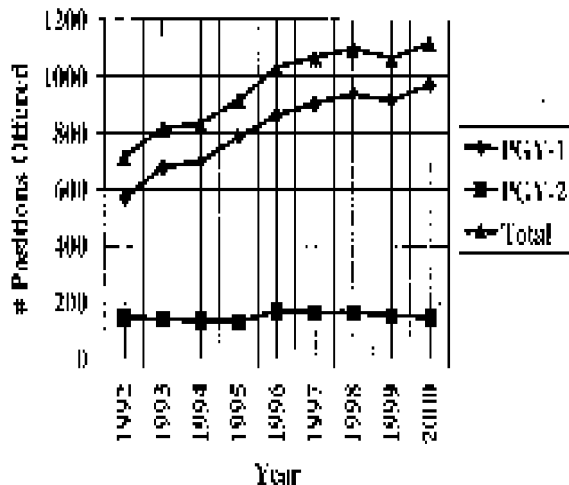


Fig. 11 Comparison of protruded surface data with Eqs. (1) and (2).

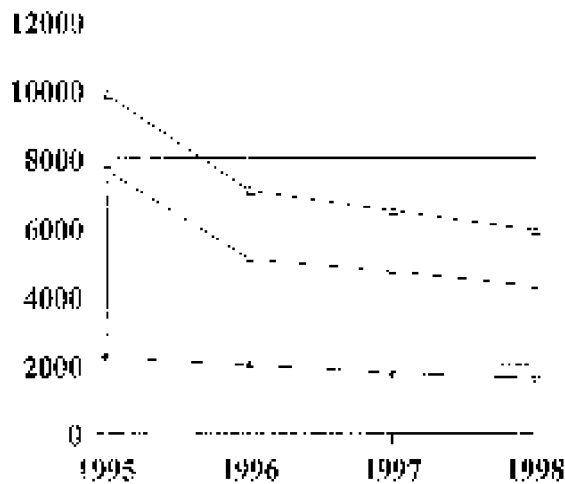


Fig. 12 Comparison of protruded surface data with Eqs. (1), (2), and (4).

height  $h_p$  for their correlation. Based on extensive experimental data, Roeller and Webb derived the following correlation:

$$\overline{Nu} = 0.150 Re^{0.632} (1 - w_p h_p / wh)^{-0.455} (h/l_p)^{-0.727} \quad (3)$$

For the present geometry,  $w_p$  and  $l_p$  are equivalent to the heated length  $L$ . This form proved to be very unsuccessful in correlating the data. Through much trial and error, the following correction was found to correlate the data with reasonable success:

$$\varepsilon_p = 1 + (h_p/D_h)^{0.428} [(h_p/D_h)^{3.048} Re^{0.794} - 1.570] \quad (4)$$

This correction to Eqs. (1) and (2) fit the protruded surface data with a mean absolute error of 11.4%. Figure 12 shows the results of the preceding effort. While the relative difference of a flush and nonflush surface CHF is dependent on subcooling, any attempt to add subcooling to the preceding correction was met with failure. However, Fig. 12 indicates that there is some slight dependence on subcooling. The reason for this difficulty is that the combination of the last term in the denominator of Eq. (2) and the density ratio generally account for subcooling in boiling correlations. This term is derived by assuming that an active layer of fluid near the surface is responsible for the accumulation of sensible and latent heat with a constant ratio between the portion of fluid evaporated and the portion that is only sensibly heated. Because of the com-

plex flow pattern about the protruded surface and the different conditions existing on the different faces, this ratio additionally becomes a function of the protrusion height and Reynolds number.

## Conclusions

1) CHF decreases with heater wall thickness and effusivity. In light of this, nonuniform heat generation for low thermal effusivity chip substrates should be considered in a chip-cooling design that employs boiling heat transfer.

2) Large-scale roughness has an effect similar to small protrusion height and causes a marked reduction of CHF.

3) For the thin foil heater, CHF is improved at velocities greater than 1 m/s for  $h_p = 0.71$  mm. A redeveloping velocity boundary layer yields higher velocity fluid tangential to the top surface and, thus, more effective liquid supply to the surface. This indicates that front-face boiling for the copper block impedes liquid supply and, consequently, reduces CHF.

4) Thin foil heater results display evidence that the instability condition at  $\Delta T_{\text{sub}} = 20^\circ\text{C}$  and  $U = 2$  m/s for the copper block is caused by the interaction of vapor emanating from the front face and boiling on the top surface. Full or partial elimination of boiling from the front face of the copper block prohibits the boiling instability at  $\Delta T_{\text{sub}} = 20^\circ\text{C}$  and  $U = 2$  m/s.

5) Full or partial elimination of boiling from the front face of the copper block increases CHF for  $U = 1$  m/s but reduces CHF for  $U \geq 2$  m/s. Results for the 0.305-mm-thick insulator show that the negative effects of the 0.635-mm-thick insulator for  $U \geq 2$  m/s may be reduced by making the insulator thinner while still preventing occurrence of the instability. Results for  $h_p < 0.635$  mm indicate that an insulator thickness less than 0.305 mm may be optimal. An optimal shape and spanwise coverage may also exist.

6) The interaction of vapor emanating from the front face and boiling from the top surface has a strong impact on increasing CHF for the case of no insulator and  $U > 2$  m/s. Condensing vapor above the surface may induce flow from the sides to yield improved liquid supply to the downstream area of the top surface.

7) As compared to the flush condition and  $U > 2$  m/s, the relative change in CHF is less for higher subcooling. This may be because of the higher contribution of single-phase heat transfer and consequent reduction in vapor interaction.

8) For all cases of the 0.635-mm protruded copper block, power dissipation is equal or improved over the flush condition. Thus, the concern for maintaining chips flush with the flow channel wall is unnecessary under certain conditions. The implications are simpler integration of direct immersion cooling with increased power dissipation. An insulator may be desired if the design specifies  $U \leq 2$  m/s.

9) A correction for protrusion height was obtained for the flush surface correlation. This correction, Eq. (4), fit the data with moderate success, the mean absolute error being 11.4%.

## Acknowledgments

This effort was supported by U.S. Air Force laboratory funds. Other support was received from the University of Kentucky. The authors wish to thank Donald P. Brigner and John E. Tennant for their diligent efforts in acquiring data and assembling the test apparatus.

## References

- Leland, J. E., Price, D. C., Hill, B. P., and Collicott, H. E., "Cooling Down Hot New Electronics," *Aerospace America*, Vol. 33, No. 6, 1995, pp. 40–44.
- Incropera, F. P., "Convection Heat Transfer in Electronic Equipment Cooling," *Journal of Heat Transfer*, Vol. 110, No. 4, 1988, pp. 1097–1111.
- Bar-Cohen, A., "Thermal Management of Air- and Liquid-Cooled Multichip Modules," *IEEE Transactions on Components, Hybrids, and Manufacturing Technology*, Vol. 10, No. 2, 1987, pp. 159–175.

<sup>4</sup>Chu, R. C., "Heat Transfer in Electronic Systems," *Proceedings of the 8th International Heat Transfer Conference*, Vol. 1, Hemisphere, New York, 1986, pp. 293-305.

<sup>5</sup>Nakayama, W., and Bergles, A. E., "Cooling Electronic Equipment: Past, Present, and Future," *Proceedings of the International Symposium on Heat Transfer in Electronic and Microelectronic Equipment*, International Centre for Heat and Mass Transfer, Dubrovnik, Yugoslavia, 1988, pp. 1-37; also *Heat Transfer in Electronic and Microelectronic Equipment*, Hemisphere, New York, 1990, pp. 1-37.

<sup>6</sup>Mudawar, I., and Maddox, D. E., "Critical Heat Flux in Subcooled Flow Boiling of Fluorocarbon Liquid on a Simulated Electronic Chip in a Vertical Rectangular Channel," *International Journal of Heat and Mass Transfer*, Vol. 32, No. 2, 1989, pp. 379-394.

<sup>7</sup>Samant, K. R., and Simon, T. W., "Heat Transfer from a Small Heated Region to R-113 and FC-72," *Journal of Heat Transfer*, Vol. 111, No. 4, 1989, pp. 1053-1059.

<sup>8</sup>Mudawar, I. A., Incropera, T. A., and Incropera, F. P., "Boiling Heat Transfer and Critical Heat Flux in Liquid Films Falling on Vertically-Mounted Heat Sources," *International Journal of Heat and Mass Transfer*, Vol. 30, No. 10, 1987, pp. 2083-2095.

<sup>9</sup>Gu, C. B., Chow, L. C., and Beam, J. E., "Flow Boiling in a Curved Channel," *Heat Transfer in High Energy/High Heat Flux Applications*, HTD-Vol. 119, American Society of Mechanical Engineers, New York, 1989, pp. 25-32.

<sup>10</sup>Leland, J. E., and Chow, L. C., "Forced Convection Boiling from a Non-Flush Simulated Electronic Chip," *Journal of Thermophysics and Heat Transfer*, Vol. 7, No. 4, 1993, pp. 588-594.

<sup>11</sup>Leland, J. E., "The Effects of Channel Curvature and Protrusion Height on Nucleate Boiling and the Critical Heat Flux of a Simulated

Electronic Chip," Ph.D. Dissertation, Univ. of Kentucky, Lexington, KY, 1994.

<sup>12</sup>McGillis, W. R., Carey, V. P., and Strom, B. D., "Geometry Effects on Critical Heat Flux for Subcooled Convective Boiling From an Array of Heated Elements," *Journal of Heat Transfer*, Vol. 113, No. 2, 1991, pp. 463-471.

<sup>13</sup>Gersey, C. O., and Mudawar, I., "Nucleate Boiling and Critical Heat Flux from Protruded Chip Arrays During Flow Boiling," *Journal of Electronic Packaging*, Vol. 115, No. 1, 1993, pp. 78-88.

<sup>14</sup>Kline, S. J., and McClintock, F. A., "Describing Uncertainties in Single-Sample Experiments," *Mechanical Engineering*, Vol. 75, Jan. 1953, pp. 3-8.

<sup>15</sup>Kenning, D. B. R., "Wall Temperature Patterns in Nucleate Boiling," *International Journal of Heat and Mass Transfer*, Vol. 35, No. 1, 1992, pp. 73-85.

<sup>16</sup>Haramura, Y., and Katto, Y., "A New Hydrodynamic Model of Critical Heat Flux, Applicable Widely to Both Pool and Forced Convection Boiling on Submerged Bodies in Saturated Liquids," *International Journal of Heat Mass Transfer*, Vol. 26, No. 3, 1983, pp. 389-399.

<sup>17</sup>Sharp, R. R., "The Nature of Liquid Film Evaporation During Nucleate Boiling," NASA Rept. TN D-1997, Oct., 1964.

<sup>18</sup>Leland, J. E., and Chow, L. C., "Channel Height and Curvature Effects on Flow Boiling from an Electronic Chip," *Journal of Thermophysics and Heat Transfer*, Vol. 9, No. 2, 1995, pp. 292-301.

<sup>19</sup>Roeller, P. T., and Webb, B. W., "A Composite Correlation for Heat Transfer from Isolated Two- and Three-Dimensional Protrusions in Channels," *International Journal of Heat and Mass Transfer*, Vol. 35, No. 4, 1992, pp. 987-990.